Progress In Electromagnetics Research Letters, Vol. 36, 9–19, 2013

ARTIFICIAL MAGNETIC CONDUCTORS ON WIDE-BAND PATCH ANTENNA

Gnanam Gnanagurunathan[1, *] and Krishnasamy T. Selvan[2]

[1]Department of Electrical and Electronic Engineering, The University of Nottingham Malaysia Campus, Selangor Darul Ehsan 43500, Malaysia

[2]Department of Electronics and Communication Engineering, SSN College of Engineering, Kalavakkam 603110, India

Abstract—The use of Artificial Magnetic Conductor (AMC) as a reflector in a printed antenna is known to improve the antenna's radiation characteristics. This work investigates the implementation of AMC as a reflector on a wideband planar monopole antenna. The investigation is confined to a basic square unit cell of AMC with four possible variations. The AMC structures are constructed with square cells which have either similar square cells or a Perfect Electric Conductor (PEC) as the back plane. These same structures are also fabricated with vias. The impedance bandwidth, gain and power pattern are simulated and measured over the measured −10 dB impedance bandwidth of 3 GHz to 10 GHz. The outcome of the investigation is that, for the antenna element and AMC structures considered in this study, a gain enhancement of up to 6 dB can be achieved with the AMC structures. In addition, introduction of vias is observed not to influence gain, though it improves cross-polarization levels by 3 dB to 5 dB for AMC constructed of squares backed by PEC.

1. INTRODUCTION

An Electromagnetic Bandgap (EBG) structure can be defined as fabricated periodic elements that may hinder, allow or confine electromagnetic waves propagation within a specified span of frequencies [1]. These structures are formed by arranging dielectric material and metallic conductors periodically. When plane waves are

Received 25 September 2012, Accepted 1 November 2012, Scheduled 7 November 2012

* Corresponding author: Gnanam Gnanagurunathan (gnanam.gnanagurunathan@nottingham.edu.my).

incident upon an EBG structure, the reflection coefficient phase varies with frequency. At a particular frequency, the incident wave encounters a reflection phase of zero degrees. At this frequency the EBG functions as an Artificial Magnetic Conductor (AMC). This structure when integrated onto a microstrip antenna below the radiating patch functions either as a reflector or as an artificial ground plane [2].

AMCs are used in low-profile microstrip antennas to generally improve their gain and bandwidth [3, 4] and directivitity [5]. Usually AMC cells are fabricated as periodic structures. However in [6], a multi periodic AMC structure is used to improve gain and also to widen the impedance bandwidth of a planar antenna. In [7], a periodic AMC structure is designed by using genetic algorithm is found to improve the bandwidth of a wideband planar antenna.

Sidelobe suppression is also possible with AMC structures as investigated in [8]. In addition, AMC can also be implemented in a resonance cavity antenna as a ground plane to achieve profile reduction by almost one-half, while maintaining high gain performance [9, 10]. Radar Cross-Section reduction can also be achieved by combining two AMCs which have overlapping bandwidths [11].

These promising improvements on the characteristics of low profile planar antennas have triggered various investigations on the possible geometries which form the AMC structure. The mushroom like EBG, when compared with uniplanar compact EBG (UC-EBG), has been found to exhibit broader bandwidth and improved gain [12]. Single, double and four arm spirals based EBG are investigated in [13] and it is reported that the four-arm spiral EBG eliminates cross-polarization effectively.

In this work, investigations are done on the performance of a wideband monopole antenna integrated with various configurations of artificial magnetic conductors. Four variations of the AMC structure, all derived from the fundamental square unit cell, are considered. The square unit cell is designed by forming the same square cell or a full PEC on the back plane of the AMC structure. The AMCs investigated are:

- square cells backed by PEC without vias (henceforth designated AMC_sq_PEC),
- square cells backed by PEC with vias (AMC_sq_PEC_vias),
- square cells backed by square cells without vias (AMC_sq_swich),
- square cells backed by square cells with vias (AMC_sq_swich_vias).

The impedance bandwidth, gain and power pattern are measured and simulated over the ultra-wideband frequency range of 3 GHz

to 10 GHz. All the simulations are done on the commercial electromagnetic simulator CST Microwave Studio.

2. ANTENNA DESIGN AND AMC CHARACTERIZATION

A wideband microstrip fed monopole antenna is designed and simulated with the same geometric configuration as in [14] (except for the band-notch slot). This design is further optimized with greater substrate thickness to enhance the impedance bandwidth. The antenna is designed using RO4350B substrate. The material dielectric constant is 3.66 and thickness is 1.524 mm. The metal thickness is 0.017 mm.

The simulated reflection co-efficient (S_{11}) of this wideband antenna is plotted in Fig. 1. The -10 dB impedance bandwidth is seen to range from 3 GHz up to 14 GHz. Based on this impedance bandwidth, the four AMC structures (i.e., AMC_sq_PEC, AMC_sq_PEC_vias, AMC_sq_swich and AMC_sq_swich_vias) are designed to have a centre frequency of about 9 GHz.

In order to determine the reflection phase of an AMC structure, the FDTD (Finite Difference Time Domain) method is employed. The reflection phase is dependent on frequency, whereby the phase reflection varies from $-180°$ to $+180°$ as the frequency increases. The scattered fields from an ideal PEC and an EBG surface are observed. The reflected phase from the EBG structure is then normalized to the reflected phase of the PEC surface. A π factor is then added to

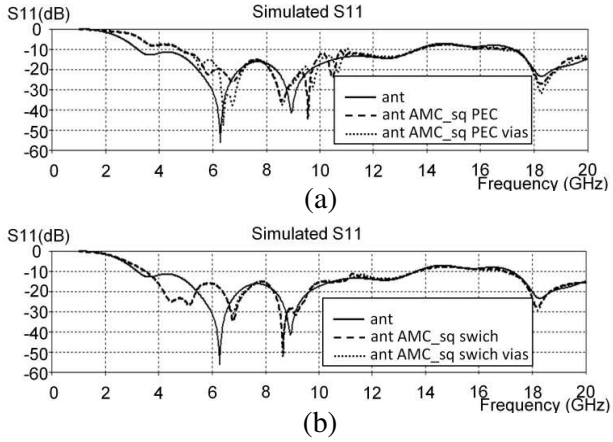

Figure 1. Simulated reflection coefficient of wideband antenna with (a) AMC_sq_PEC with and without vias and (b) AMC_sq_swich with and without vias.

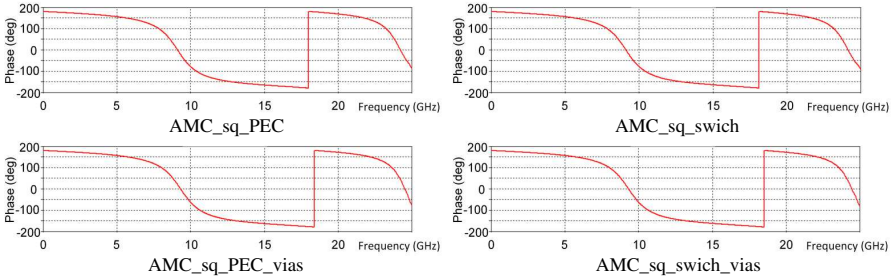

Figure 2. Simulated reflection phase for the AMC structures.

the phase result to account for the reference of a PEC surface [1]. A single AMC cell is simulated and characterized in order to reproduce a structure which is periodic and infinite.

The AMC dimensions are parametrically analyzed to have 0 degree phase reflection at 9 GHz. The material used is the same as the wideband antenna. The unit cell of the AMC has a metal patch size of 6.5 mm × 6.5 mm. The gap between the patches is 2 mm. The vias radius is 0.5 mm. The AMC grid is formed by 5 × 4 unit cells. The number of unit cells has been chosen to give optimal performance with a small profile. The simulated reflection phases for a normally incident plane wave for all the four AMC are shown in Fig. 2. All the four variations of AMC display similar phase reflection characteristics centered at 9 GHz.

The AMCs are then integrated onto a wideband monopole antenna. They are spaced at $\lambda/4$ (at 9 GHz) away from the ground plane of the monopole antenna. This spacing was arrived at by undertaking a parametric analysis on the space between the wideband monopole and one of the AMC structures, i.e., AMC_sq_PEC whereby optimal −10 dB bandwidth and antenna performance is obtained. For additional verification the intensity of the electrical field on the AMC structure at varying space is observed and shown in Fig. 3. The E-field intensity is strongest at a spacing of 9 mm and lesser. Thus, the spacing for all the four AMC structures is maintained at 9 mm for simulation and measurements. At this spacing the incidental E-field is reflected constructively, thereby enabling the AMC to function as a reflector.

The simulated impedance bandwidth of antennas with and without AMC are shown in Fig. 1. Improvement in −10 dB impedance bandwidth by almost 1 GHz is noted for the AMC_sq_swich and AMC_sq_swich_vias in comparison to the wideband antenna without AMC. However, the impedance bandwidth remains almost the same for the AMC_sq_PEC and AMC_sq_PEC_vias as for the antenna without

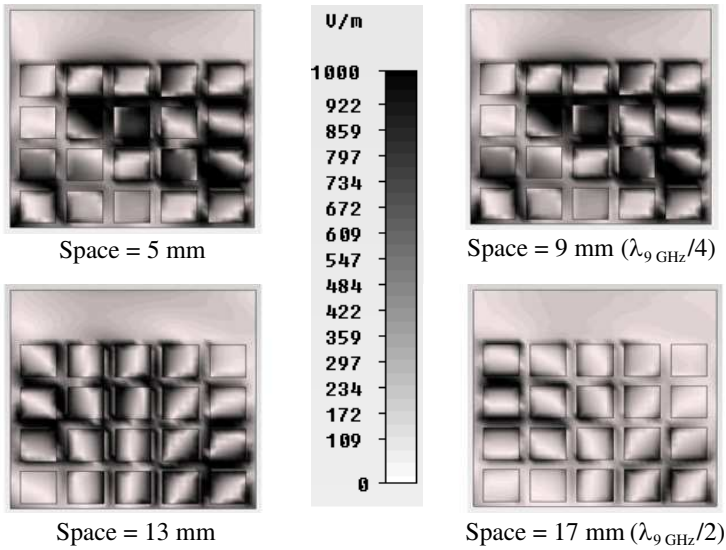

Figure 3. *E*-field intensity on the AMC_sq_PEC. The intensity is shown for differing distance between AMC and wideband antenna.

AMC. The wideband antenna and the AMC structures are fabricated as shown in Fig. 4 and measured for reflection co-efficient (S_{11}), radiation pattern and gain.

3. PERFORMANCE OF THE AMC INTEGRATED ANTENNA

The measured impedance bandwidth for the wideband monopole antenna with and without the AMC reflectors are shown in Fig. 5. The wideband antenna's measured impedance bandwidth spans from 4 GHz up to 8 GHz. The variation in the measured impedance bandwidth compared to simulation prompted a second fabrication of the wideband monopole antenna, in order to rule out the possibility of gross fabrication errors causing the variation. The second antenna too displayed similar impedance bandwidth as the first one. It is observed from simulation and measurement that the impedance bandwidth of the antenna with AMC is similar to that of the antenna without it. Therefore, radiation pattern and gain measurements were carried out over a frequency range of 3 GHz to 10 GHz which is in fact the UWB frequency range.

During measurement, the impedance bandwidths of AMC_sq_PEC

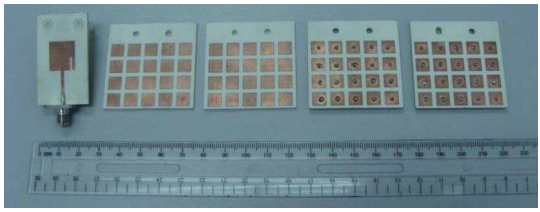

(a)

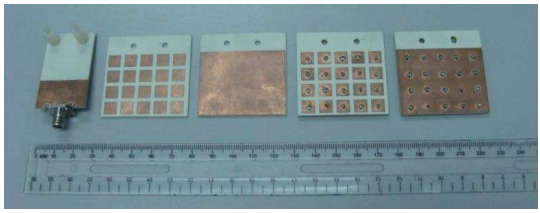

(b)

Figure 4. Fabricated wideband antenna and the four AMC structures, (a) front profile and (b) back profile.

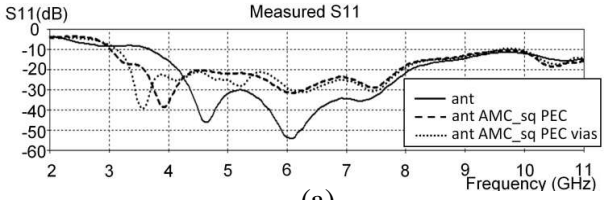

(a)

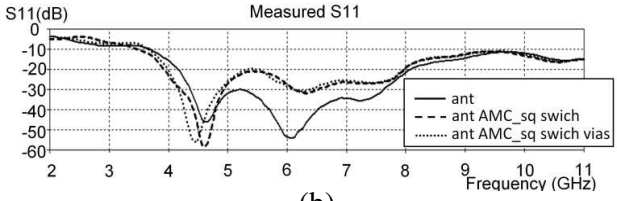

(b)

Figure 5. Measured reflection co-efficient of wideband antenna with (a) AMC_sq_PEC with and without vias and (b) AMC_sq_swich with and without vias.

and AMC_sq_PEC_vias improve by almost 1 GHz in the lower band. No significant bandwidth improvement is noted with the AMC_sq_swich and AMC_sq_swich_vias, unlike the simulation. Therefore a significant improvement in the bandwidth could not be concluded. The simulated gain is plotted in Fig. 6. Significant gain improvement is noted with the AMC reflectors.

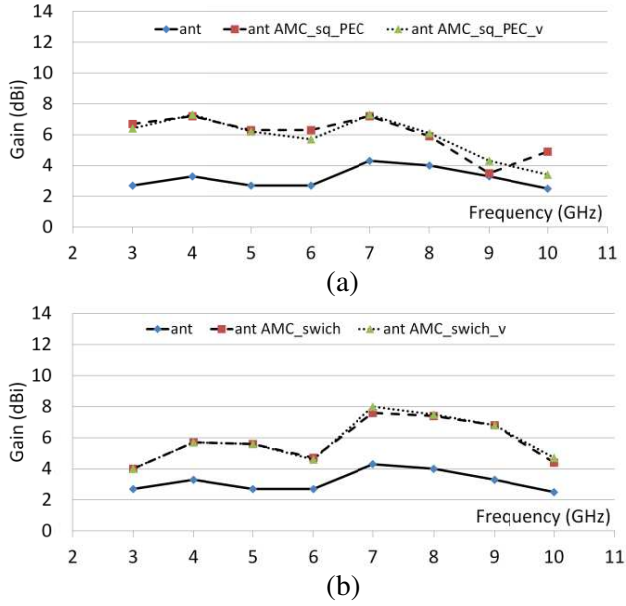

Figure 6. Simulated gain of wideband antenna with AMC reflectors with and without vias for (a) AMC_sq_PEC and (b) AMC_sq_swich.

The peak gain in the forward radiation hemisphere is then measured using the three antenna method in the university's antenna test facility. Gain measurement is carried out in 3 GHz to 10 GHz frequency range at 1 GHz interval, and the values are plotted in Fig. 7. Significant gain improvement is observed over the wideband frequencies for all the four variations of the AMC structures. The improvement in gain is not influenced by the presence of vias, as similar gain improvement is observed for AMC with or without vias. The AMC_sq_PEC and AMC_sq_PEC_vias show gain improvement over the entire observed range of frequency. On the other hand the gain improvement of AMC_sq_swich and AMC_sq_swich_vias is only from 5 GHz up to 10 GHz.

The improvement in gain is due to the positioning of the AMC structures as reflectors. Incidental waves from the radiating patch that come in contact with the AMC structures are reflected in phase. Although the AMC is designed at a centre frequency of 9 GHz (based on the simulation outcomes), the improvement in gain is significant ranging from 1 dB up to almost 6 dB over the entire range of the measured −10 dB impedance bandwidth.

The co- and cross-polarized radiation patterns in the frequency range of 3 GHz to 10 GHz range at an interval of 1 GHz are measured for all the antenna configurations. In view of space constraints,

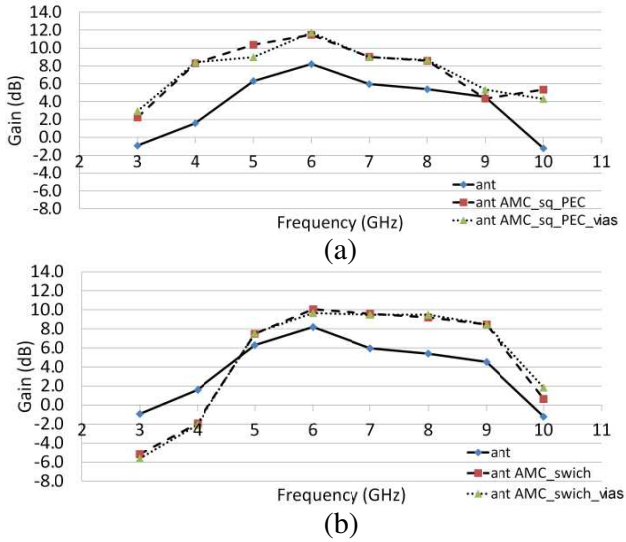

Figure 7. Measured gain of wideband antenna with AMC reflectors with and without vias for (a) AMC_sq_PEC and (b) AMC_sq_swich.

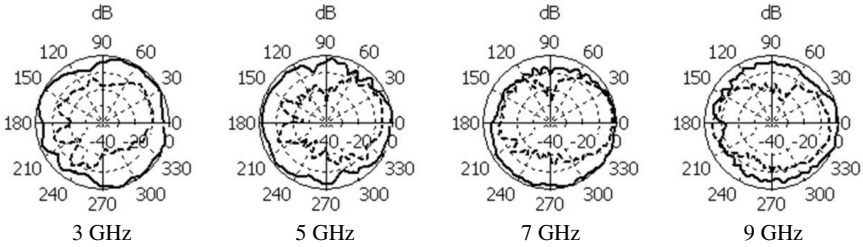

Figure 8. Radiation pattern of the wideband patch antenna (co-polarized: solid line and cross-polarized: dotted line).

Fig. 8 through Fig. 12 depicts the radiation patterns only at some of the frequencies. In Fig. 8 the wideband monopole antenna's radiation pattern is shown for all the odd frequencies. While the radiation pattern of the wideband antenna without AMC is almost omnidirectional, the integration of the AMC ground planes makes it more directional thus resulting in gain improvement.

Cross polarization exists for almost all the frequencies. However, in the case of the AMC_sq_PEC_vias a significant suppression of almost 3 dB to 5 dB in the cross polarization level is noted compared to the AMC_sq_PEC. The radiation pattern of antenna with AMC_sq_PEC and AMC_sq_PEC_vias at the frequencies of 4 GHz, 5 GHz, 8 GHz and

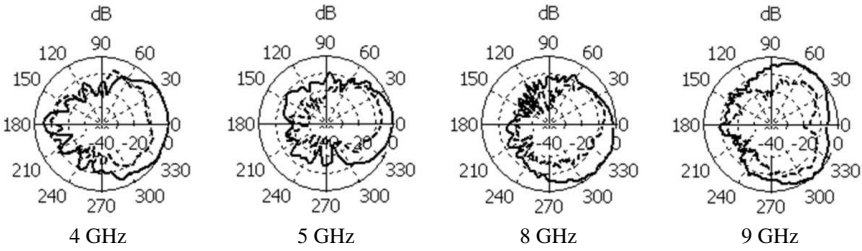

Figure 9. Radiation pattern of the wideband patch antenna and AMC_sq_PEC (co-polarized: solid line and cross-polarized: dotted line).

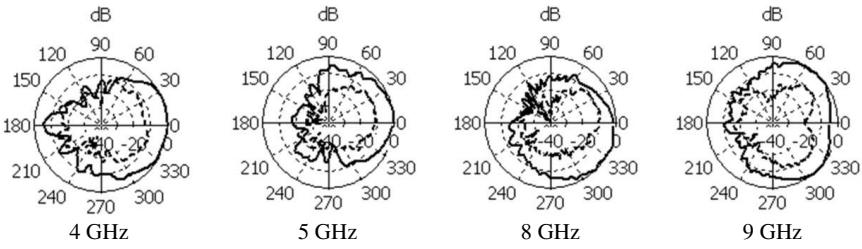

Figure 10. Radiation pattern of the wideband patch antenna and AMC_sq_PEC_vias (co-polarized: solid line and cross-polarized: dotted line).

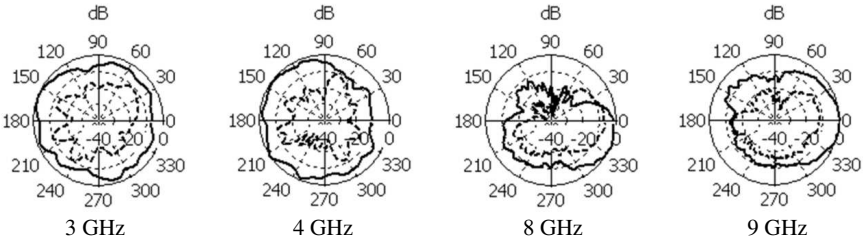

Figure 11. Radiation pattern of the wideband patch antenna and AMC_sq_swich (co-polarized: solid line and cross-polarized: dotted line).

9 GHz highlight significant suppression of the cross polarization as shown in Figs. 9 and 10. Generally the cross polarization levels of the antenna with AMC are lower compared to wideband antenna without AMC.

Meanwhile the antenna with AMC_sq_swich and AMC_sq_swich_vias radiation patterns are plotted for 3 GHz, 4 GHz, 8 GHz and 9 GHz frequency as shown in Figs. 11 and 12. The 3 GHz and 4 GHz

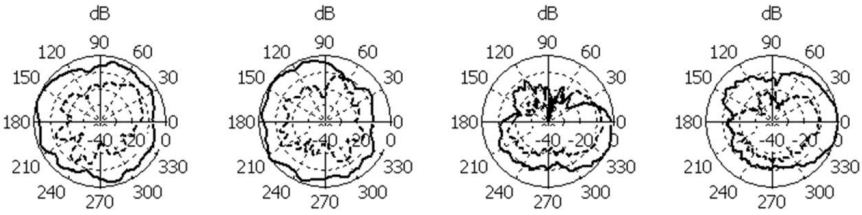

Figure 12. Radiation pattern of the wideband patch antenna and AMC_sq_swich_vias (co-polarized: solid line and cross-polarized: dotted line).

radiation patterns indicate stronger backward radiation. This is also reflected in the forward gain computation which shows a drop at these frequencies compared to the wideband antenna without AMC.

4. CONCLUSION

In this work, the following variations of an AMC structure, placed as reflectors on a wideband monopole antenna were investigated: square cells backed by square cells — with and without vias and square cells backed by a Perfect Electric Conductor (PEC) — with and without vias. Despite displaying similar reflection phase characteristics, the AMCs performance when integrated with wideband antenna differed. Generally gain improvement was noted with all the AMC structures. It was also noted that the introduction of the vias does not influence the gain. Cross polarization levels improved by 3 dB to 5 dB with AMC which had squares backed by PEC with vias. Therefore, it is concluded that AMC structures with same reflection phase characteristics could exhibit different performance when integrated with the antenna.

REFERENCES

1. Yang, F. and Y. Rahmat-Samii, *Electromagnetic Bandgap Structures in Antenna Engineering*, Cambridge University Press, 2009.
2. Sievenpiper, D., L. Zhang, R. F. J. Broas, N. G. Alexopolous, and E. Yablonovitch, "High-impedance electromagnetic surfaces with a forbidden frequency band," *IEEE Transactions on Microwave Theory and Techniques*, Vol. 47, No. 11, 2059–2074, 1999.
3. Qu, D., L. Shafai, and A. Foroozesh, "Improving microstrip patch antenna performance using EBG substrates," *IEE Proceedings on Microwaves, Antennas and Propagation*, Vol. 153, 558–563, 2006.

4. Elsheakh, D. A., H. A. Elsadek, E. A. Abdallah, H. Elhenawy, and M. F. Iskandar, "Enhancement of microstrip monopole antenna bandwidth by using EBG structures," *IEEE Antennas and Wireless Propagation Letters*, Vol. 8, 959–962, 2009.
5. De Cos, M. E., Y. Alvarez-Lopez, and F. Las-Heras, "On the influence of coupling AMC resonances for RCS reduction in the SHF band," *Progress In Electromagnetics Research*, Vol. 117, 103–119, 2011.
6. C. C. Chiau, X. Chen, and C. Parini, "Multiperiod EBG structure for wide stopband circuits," *IEE Proceedings on Microwaves, Antennas and Propagation*, Vol. 150, 489–492, 2003.
7. Akhoondzadeh-Asl, L., D. J. Kern, P. S. Hall, and D. H. Werner, "Wideband dipoles on electromagnetic bandgap ground planes," *IEEE Transactions on Antennas and Propagation*, Vol. 55, No. 9, 2426–2434, 2007.
8. Zhang, Y., J. von Hagen, M. Younis, C. Fischer, and W. Wiesbeck, "Planar artificial magnetic conductors and patch antennas," *IEEE Transactions on Antennas and Propagation*, Vol. 51, No. 10, 2003.
9. Feresidis, A. P., G. Goussetis, S. Wang, and J. C. Vardaxoglou, "Artificial magnetic conductor surfaces and their application to low-profile high-gain planar antennas," *IEEE Transactions on Antennas and Propagation*, Vol. 53, No. 1, 2005.
10. Wang, S., A. P. Feresidis, G. Goussetis, and J. C. Vardaxoglou, "Low-profile resonant cavity antenna with artificial magnetic conductor ground plane," *Electronics Letters*, Vol. 40, No. 7, 405–406, 2004.
11. Kim, S.-H., T. T. Nguyen, and J.-H. Jang, "Reflection characteristics of 1-D EBG ground plane and its application to a planar dipole antenna," *Progress In Electromagnetics Research*, Vol. 120, 51–66, 2011.
12. Sohn, J. R., K. Y. Kim, H.-S. Tae, and H. J. Lee, "Comparative study on various artificial magnetic conductors for low-profile antenna," *Progress In Electromagnetics Research*, Vol. 61, 27–37, 2006.
13. Kim, Y., F. Yang, and A. Z. Elsherbeni, "Compact artificial magnetic conductor designs using planar square spiral geometries," *Progress In Electromagnetics Research*, Vol. 77, 43–54, 2007.
14. Chung, K., J. Kim, and J. Choi, "Wideband microstrip-fed monopole antenna having frequency band-notch function," *IEEE Microwave and Wireless Components Letters*, Vol. 15, No. 11, 766–768, 2005.